

# Thermal consequences of sintering the borosilicate matrix blue-green color release properties

Ha Thanh Tung<sup>1</sup>, Dieu An Nguyen Thi<sup>2</sup>

<sup>1</sup>Faculty of Basic Sciences, Vinh Long University of Technology Education, Vinh Long City, Vietnam

<sup>2</sup>Faculty of Electrical Engineering Technology, Industrial University of Ho Chi Minh City, Ho Chi Minh City, Vietnam

## Article Info

### Article history:

Received Nov 1, 2022

Revised Nov 28, 2022

Accepted Dec 21, 2022

### Keywords:

Color rendering indexes

Illumination effectiveness

Phosphors

White illumination

White light emitting diodes

## ABSTRACT

Color transformation glass ceramics were produced of borosilicate matrix co-doped (SrBaSm)Si<sub>2</sub>O<sub>2</sub>N<sub>2</sub>:(Eu<sup>3+</sup>Ce<sup>3+</sup>) blue-green (B-G) (abbreviated as (SBS)SON:(EuCe) B-G) phosphors using a two-step co-sintering technique. The shift in illumination characteristics and drift of chromaticity coordinates (CIE) of (SBS)SON:(EuCe) (B-G) phosphors and hue transformation glass ceramics were investigated over a 600–800 °C sintering thermal range. With rising sintering heat, the illuminated strength and inner quantum yield (QY) of (abbreviated as B-G) phosphors and glass ceramics reduced. Once the sintering heat was raised above 750 °C, the phosphors and hue transformation glass ceramics showed nearly no high point among their luminescence photoluminescence (PL) and photoluminescence excitation (PLE) bands of color. B-G phosphors have low heating steadiness at more elevated temperatures, according to the findings. The glass matrix destructed the phosphors lattice layout and the Ce<sup>3+</sup> in the phosphors was oxidized to Ce<sup>4+</sup>, resulting in a reduction in the luminous characteristics of the color transformation glass ceramics.

This is an open access article under the [CC BY-SA](https://creativecommons.org/licenses/by-sa/4.0/) license.



## Corresponding Author:

Dieu An Nguyen Thi

Faculty of Electrical Engineering Technology, Industrial University of Ho Chi Minh City

Ho Chi Minh City, Vietnam

Email: nguyenthidieu@iuh.edu.vn

## 1. INTRODUCTION

During a period when power is becoming rare, diodes emit white illumination white light emitting diodes (WLEDs) has sparked intense interest in a variety of areas due to their elevated effectiveness, energy savings, impact resistance, long lifespan, environmental protection, and quick reaction [1]–[3]. Even so, as technology advances, WLEDs with just superior efficiency will no longer be able to fulfill consumer needs. Full-spectrum WLEDs, which have greater color rendering indexes (CRI), greater illumination effectiveness, and better color reproduction capability than sunlight, have been used to resolve the issue of too much blue light destruction [4], [5]. In comparison to general WLEDs, full-spectrum WLEDs are typically synthesized by including phosphors of 490 nm and 660 nm to supplement near-wave blue-green (B-G) illumination and lengthy-wave red illumination, leading to the spectral wavelength encompasses all visible light [6], [7]. Phosphors with a wavelength of 660 nm are currently being researched thoroughly [8]–[10]. As a result, the 490 nm range of B-G phosphor is a critical matter in the study and setting up of filled-spectrum light emitting diodes (LEDs). Several B-G phosphors, such as silicate (M<sub>2</sub>SiO<sub>4</sub>:Eu<sup>2+</sup>, M=Ca, Ba, Sr), sulfide (M<sub>2</sub>BS<sub>4</sub>:Eu<sup>2+</sup>, M=Ba, Sr, Ca, B=Al, Ga, In), and aluminate (MSrAl<sub>37</sub>:Eu<sup>2+</sup>, M=Y, La, Gd) are presently being established [11], [12]. The conventional silicate structure, on the other side, has a limited emission maximum and poor color rendering traditional sulfide phosphors typically have poor stability, sensitivity to surrounding humidity and ambiance, aluminate is hard to compound, expensive, and prone to hydrolysis [13]. System of

oxynitride-based phosphors such as (SBS)SON:(EuCe) B-G phosphor materials have high benefits in study because they have many benefits such as increased illuminated effectiveness, efficient stimulation using viewable illumination, elevated performance factor of fluorescent features (broad modification scope), elevated heating steadiness, and environmental protection. Instead, the processing method of packet-filled WLEDs bands of color must conquer silicone's easy aging and yellowing [14]. Many color transformation glass ceramics for WLEDs works are being completed both domestically and overseas. At the moment, the glass materials utilized in color transformation glass ceramic study are primarily glass matrices of bismuthate, tellurate, and borosilicate. When there is a comparison between glass matrix materials, the borosilicate glass matrix material includes two major benefits: i) it has excellent heating stability, precludes the phosphor from having failed under rising temperature, and high moisture and ii) it is relatively steady, allowing glass ceramics with many-wavelength phosphor doping to be realized. As a result, the characteristics of borosilicate matrix B-G color transformation glass ceramics must be investigated [15], [16].

Hue transformation glass ceramics were created by sintered borosilicate glass matrix and B-G phosphors according to this investigation at a sintering heat 600–800 °C, with a retaining period of 20 minutes. The influence of sintering temperature on the illumination characteristics of B-G hue transformation glass ceramics with borosilicate matrix was investigated. The shift in photoluminescence (PL) strength at each sintering temperature allows us to evaluate the luminescence of B-G hue transformation glass ceramics. Furthermore, x-ray diffraction (XRD) can be utilized to investigate the lattice layout between phosphors and glass ceramics having different sintering heats, the content and variation of  $\text{Ce}^{3+}$  and  $\text{Eu}^{3+}$  can be assessed using the x-ray photoelectron band of color analyzer to examine the hue transformation glass ceramics' characteristics at rising sintering temperatures [17], [18].

## 2. COMPUTATIONAL SIMULATION

B-G color transformation glass ceramics could be acquired using a two-stage technique in low-heat cooperatively sintering in this procedure. To begin, the weighed and combined medicine ( $\text{H}_3\text{BO}_3$ ,  $\text{SiO}_2$ ,  $\text{ZnO}$ ,  $\text{BaCO}_3$ ,  $\text{Na}_2\text{CO}_3$  to heat the glass matrix) was sintered at 1,100 °C in a muffle furnace within one hour. Second, the clear elevated-heat fluid removed from the muffle furnace was chilled at room temperature on a copper plate. Finally, ground glass-matrix outcomes with a  $d_{50}$  of 15 m were added with 3 wt% (SBS)SON:(EuCe) B-G phosphor fine grains with a  $d_{50}$  of 15 m and put in a muffle furnace at 600–800 °C within 20 minutes [19], [20]. The prepared specimen's lattice layout can be determined using XRD for a  $2\theta$  range of 10° to 80° with Cu  $K_\alpha$  radiation ( $k=0.154178$  nm) at a scanning ratio of 0.02°/step and 4°/min. The PL, photoluminescence excitation (PLE), and quantum yield (QY) of whole specimens containing B-G phosphors and hue transformation glass ceramics were measured using a spectrofluorometer and an integrating sphere illuminated by a xenon light. Assessing the ratio of the region taken up by divalent and trivalent europium ions using x-ray photoelectron spectrum analysis software data can recommend the illumination characteristics of color transformation glass ceramics. The carbon 1 s line was utilized to verify each binding energies ( $\text{C1 s}=284.91$  eV).

## 3. RESULTS AND DISCUSSION

In this section, we compare  $\text{YAG:Ce}^{3+}$  to the six conversion phosphor requirements that we proposed. The emission spectrum of  $\text{YAG:Ce}^{3+}$  is really wide, with a typical full width at half maximum (FWHM) of 100 nm. The blue pumping LED can easily excite  $\text{YAG:Ce}^{3+}$ , with a well enough wide stimulation range closely 460 nm demonstrating great superimposed on each other with the LED's emitting bands of color. At low dopant concentrations,  $\text{YAG:Ce}^{3+}$  exhibits outstanding heat extinguishing behavior, retaining exceeding 50% in the normal heat emitting strength at 700 K. It has an elevated quantum efficiency (90% or higher), which is required for the manufacture of effective LED packages. It has superior chemical stability and does not degrade beneath the high stimulation fluxes encountered in pLEDs. Because of the permitted essence of the emitting transfer in  $\text{Ce}^{3+}$ , the radiation is rapid.

Clearly,  $\text{YAG:Ce}^{3+}$  meets all six requirements with flying colors. The biggest limitation of  $\text{YAG:Ce}^{3+}$  is a shortage in orange-red radiation of the viewable color bands. It limits the LED's improvement with elevated hue rendering and/or poor hue heat. The changed  $\text{YAG:Ce}^{3+}$  phosphors have a reduced heating extinguishing heat overall. Nevertheless, because of the breadth of the emission spectrum, a significant portion of the illumination released exceeds 650 nm. Because the eye's sensitiveness is significantly low within this area of the bands of color, the pLED general performance is reduced. As a result, including a second, strait-radiating red phosphor inside the phosphor mixture may have greater effectiveness. For greater  $\text{Ce}^{3+}$  concentrations, the radiation exhibits a (tiny) red shift, which is caused in part by reabsorption, as well as a decrease in the thermal quenching temperature. Lower dopant concentrations are thus beneficial for high

flux gadgets. The reduced absorbing efficiency might be mitigated by using clear ceramic plates for the hue transformation film, which reduces dispersion losses significantly.

Figure 1 illustrates the reverse change in dosages of green phosphorus (SBS)SON:(EuCe) and yellow phosphorus YAG:Ce<sup>3+</sup>. There are different concentrations to keep the mean correlated color temperature (CCT) value at 3,000 K, 4,000 K, and 5,000 K, as in Figures 1(a)-(c), and respectively. This shift has two meanings: the first one is to retain mean CCTs and the next one is to modify the absorptivity and scatter of lights in WLEDs dual-phosphor-film model. This ultimately impacts the WLEDs hue standard and illuminated beam effectiveness. Thus, the hue standard of WLEDs is determined by the dosage of (SBS)SON:(EuCe). When the (SBS)SON:(EuCe) concentration grew 2-20% Wt, the YAG:Ce<sup>3+</sup> dosage reduced to retain the mean CCTs. It is also true about WLEDs with hue heats ranging 5,600-8,500 K.

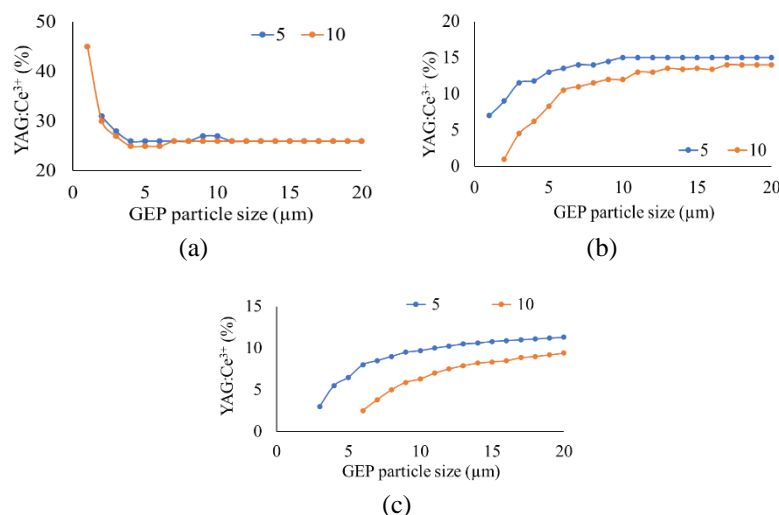


Figure 1. Adjusting the dosage of phosphor to keep the medium CCT; (a) 3,000 K, (b) 4,000 K, and (c) 5,000 K

In Figure 2, the graphs show the impact of (SBS)SON:(EuCe) green phosphorus concentration on the power of spectral transmission of WLEDs at 3,000 K Figure 2(a), 4,000 K Figure 2(b), and 5,000 K Figure 2(c). It is possible to make a decision depending on the specs provided by the manufacturer. Lighting output may be slightly reduced by WLEDs that need high color fidelity. The synthesizing of the spectral regions is white illumination, especially of the two regions 420–480 nm and 500–640 nm. It is observed that these two specific spectral areas display increasing intensity with increasing concentration (SBS)SON: (EuCe). This change in the two-band emitting bands of hues shows that the output illumination has increased. Furthermore, blue-illumination diffusing in WLEDs is raised, meaning that diffusion in the phosphor film and in WLEDs is raised, which favors hue homogeneity. When (SBS)SON:(EuCe) is applied, this is a noteworthy outcome. It is difficult to control the hue homogeneity when applying a remote-phosphor-layer setup in a WLED package with CCT>5,000 K [21]–[23]. According to this article, (SBS)SON:(EuCe) shows a high probability in enhancing the chroma quality for WLED lamps at both minimum and maximum hue heats (5,600 K and 8,500 K).

Consequently, the paper demonstrated the illumination intensity of this distant green-phosphor layer in WLEDs. The outcomes in Figures 3(a)-(c) reveals the illumination emitted dramatically increases (3,000 K–4,000 K–5,000 K) as the concentration of (SBS)SON:(EuCe) grows 2% wt-20% wt. The hue deviation was drastically declined with the phosphor (SBS)SON:(EuCe) dosage in all mean CCTs (3,000 K–4,000 K–5,000 K), as the results of Figures 4(a)-(c). This is because of the red phosphor film's absorption. When the (SBS)SON:(EuCe) phosphor absorbs blue illumination in the LED chip, the blue phosphor portions will change it to green illumination. The (SBS)SON:(EuCe) portions absorb yellow illumination in extra to the blue illumination from the LED chip. Even so, owing to the substance's absorbing properties, the absorption for blue emission is much greater the yellow one. According to the addition of (SBS)SON:(EuCe), the green illumination proportion inside WLEDs raises, leads to an advancement in the uniformity of chroma. As the chroma uniformity is a crucial factor for a good-quality WLED light, it will cost more to purchase for a greater color-uniformity-index WLED. On the other hand, the advantage when utilizing (SBS)SON:(EuCe) is its cost effective, so it is possible to have (SBS)SON:(EuCe) broadly used in production.

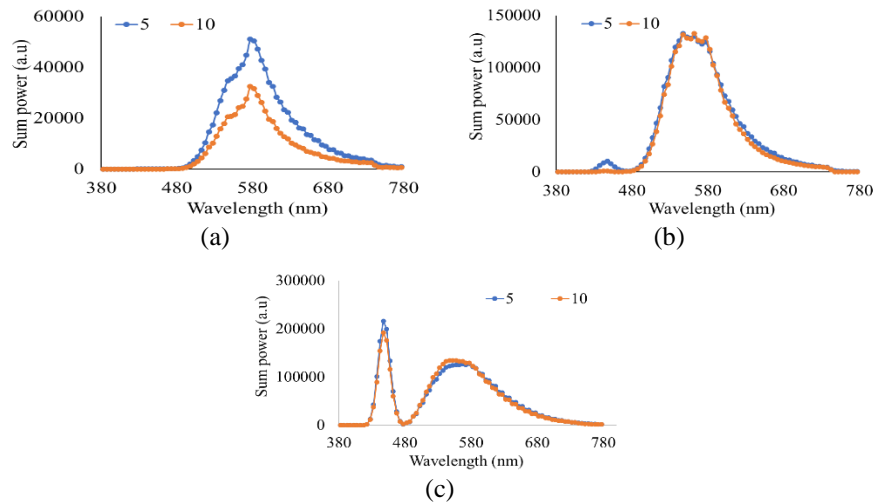


Figure 2. The emitting bands of hue of WLEDs as a function of (SBS)SON:(EuCe) dosage; (a) 3,000 K, (b) 4,000 K, and (c) 5,000 K

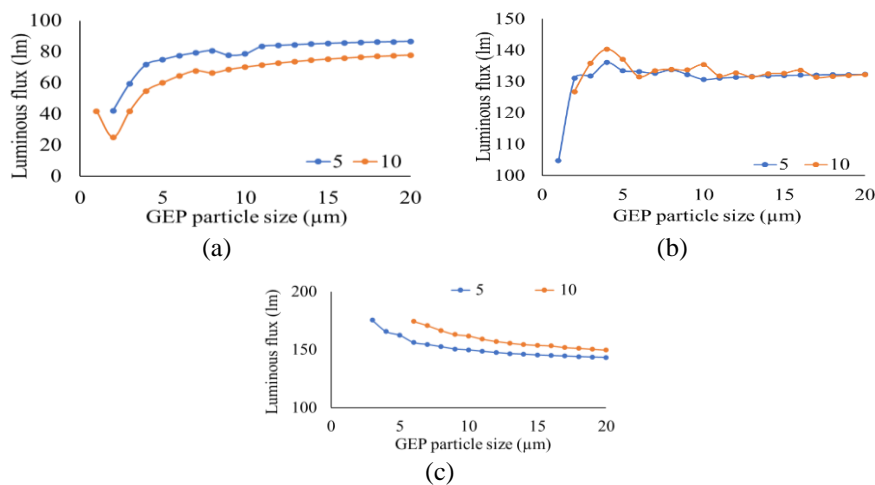


Figure 3. The lighting beam of WLEDs as a function of (SBS)SON:(EuCe) dosage; (a) 3,000 K, (b) 4,000 K, and (c) 5,000 K

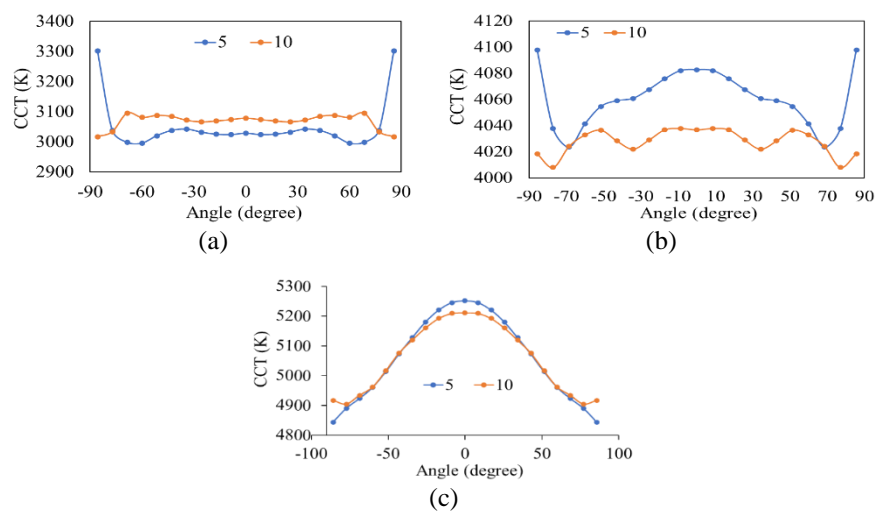


Figure 4. The CCT of WLEDs as a function of (SBS)SON:(EuCe) dosage; (a) 3,000 K, (b) 4,000 K, and (c) 5,000 K

Color homogeneity is only one factor to give thought to when assessing the WLEDs chroma standard. We cannot say the hue standard is great with just a high hue homogeneity indicator. Consequently, new research includes a hue rendition indicator CRI and chroma quality scale (CQS). The CRI identifies an object's true color when illuminated. Green illumination in excess between the fundamental hues of blue, yellow, and green is what is causing the color imbalance. WLED hue fidelity is reduced as a result of this having an effect on the hue standard of WLEDs. Figure 5 includes the graph of CRI result that shows a small decrease when integrating (SBS)SON:(EuCe) phosphor. Figures 5(a)-(c) show the CRI values according to the CCTs of 3,000 K–4,000 K–5,000 K, in turn. As a result, all of those are acceptable as CRI is only a problem with CQS. CQS is more important and harder to get when compared to CRI. CQS is a three-element indicator determined by three variables: hue rendering indicator, viewer preference, and hue coordinate, making it virtually a genuine overall parameter to evaluate the chroma adequacy and fidelity [24], [25]. CQS data based on CCT value of 3,000 K–5,000 K are illustrated in turn in Figures 6(a)-(c), in which its improvement in the presence of the remote phosphor (SBS)SON:(EuCe) layer is observed. Furthermore, when the (SBS)SON:(EuCe) concentration is elevated, CQS will not shift dramatically with (SBS)SON:(EuCe) concentrations just under 10% wt. Conversely, either CQS or CRI declined considerably when the (SBS)SON:(EuCe) portion exceeds 10% wt, as a result of severe hue-balance loss as the green hue is prominent. As a consequence, when utilizing green phosphor (SBS)SON:(EuCe), appropriate dosage selection is necessary [26]–[28].

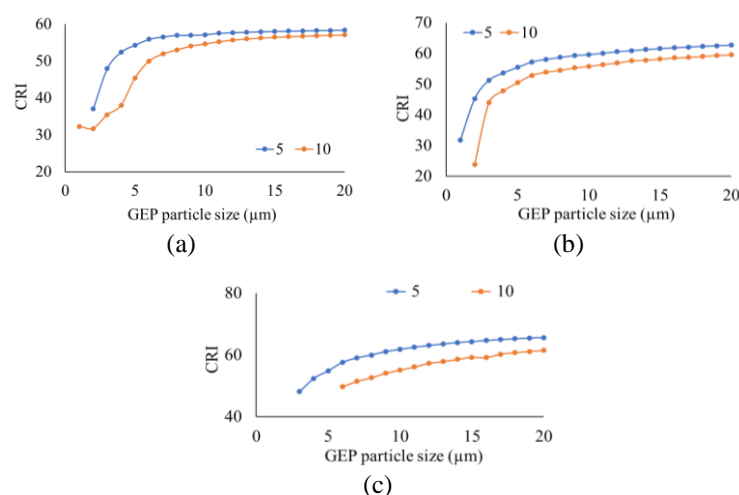


Figure 5. The WLEDs hue rendering indicator as a function of (SBS)SON:(EuCe) dosage; (a) 3,000 K, (b) 4,000 K, and (c) 5,000 K

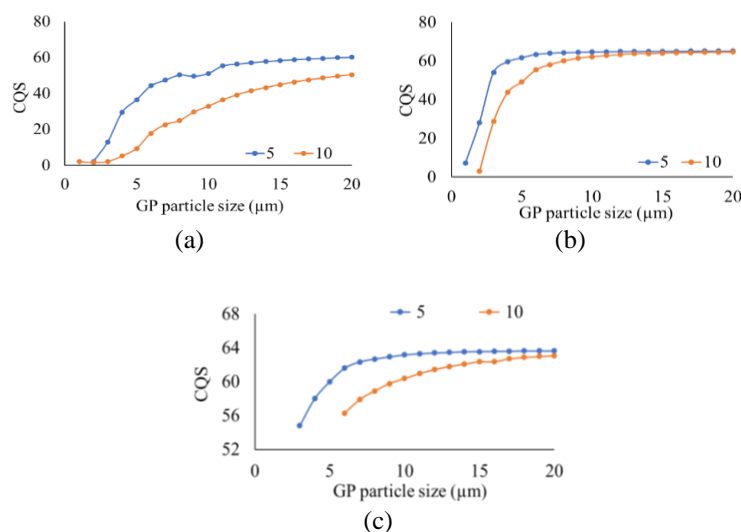


Figure 6. The hue standard scale of WLEDs as a function of (SBS)SON:(EuCe) dosage; (a) 3,000 K, (b) 4,000 K, and (c) 5,000 K

#### 4. CONCLUSION

The illumination characteristics of  $(\text{SrBaSm})\text{Si}_2\text{O}_7\text{N}_2:(\text{Eu}^{3+}\text{Ce}^{3+})$  blue–green color transformation glass ceramics shifted with sintering heat were experimentally investigated and validated via a sequence of experiments. The illuminated strength of color transformation glass ceramics progressively decreases as the sintering heat raises 600–700 °C, but they retain illumination characteristics. Once the sintering heat surpasses 750 °C, the glass ceramics illumination strength reduces linearly and reaches zero. In the meantime, the fluorescence properties of color transformation glass ceramics are nearly non-existent. At 750 °C, the B-G phosphors were pyretic extinguished. Furthermore, the glass matrix destructed the phosphors' lattice layout, and the  $\text{Ce}^{3+}$  in the phosphors was oxidized to  $\text{Ce}^{4+}$ , resulting in a decline in the luminous strength of hue transformation glass ceramics. The investigational outcomes reveal that a reduced sintering heat improves the illumination characteristics of B-G hue transformation glass ceramics.




#### REFERENCES

- [1] M. S. Wong *et al.*, “High efficiency of III-nitride micro-light-emitting diodes by sidewall passivation using atomic layer deposition,” *Optics Express*, vol. 26, no. 16, pp. 21324–21331, Aug. 2018, doi: 10.1364/oe.26.021324.
- [2] Y. Park, K. H. Li, W. Y. Fu, Y. F. Cheung, and H. W. Choi, “Packaging of InGaN stripe-shaped light-emitting diodes,” *Applied Optics*, vol. 57, no. 10, pp. 2452–2458, Apr. 2018, doi: 10.1364/ao.57.002452.
- [3] K. Gibasiewicz *et al.*, “InGaN blue light emitting micro-diodes with current path defined by tunnel junction,” *Optics Letters*, vol. 45, no. 15, pp. 4332–4335, Aug. 2020, doi: 10.1364/ol.394629.
- [4] X. Tao *et al.*, “Performance enhancement of yellow InGaN-based multiple-quantum-well light-emitting diodes grown on Si substrates by optimizing the InGaN/GaN superlattice interlayer,” *Optical Materials Express*, vol. 8, no. 5, pp. 1221–1230, 2018, doi: 10.1364/ome.8.001221.
- [5] K. H. Li *et al.*, “Monolithically integrated InGaN/GaN light-emitting diodes, photodetectors, and waveguides on Si substrate,” *Optica*, vol. 5, no. 5, pp. 564–569, May 2018, doi: 10.1364/optica.5.000564.
- [6] C. F. Fong *et al.*, “Silicon nitride nanobeam enhanced emission from all-inorganic perovskite nanocrystals,” *Optics Express*, vol. 27, no. 13, pp. 18673–18682, Jun. 2019, doi: 10.1364/oe.27.018673.
- [7] V. Ryzhii *et al.*, “Theoretical analysis of injection driven thermal light emitters based on graphene encapsulated by hexagonal boron nitride,” *Optical Materials Express*, vol. 11, no. 2, pp. 468–486, Feb. 2021, doi: 10.1364/ome.412973.
- [8] P. S. Yeh, Y.-C. Chiu, T.-C. Wu, Y.-X. Chen, T.-H. Wang, and T.-C. Chou, “Monolithic integration of GaN-based phototransistors and light-emitting diodes,” *Optics Express*, vol. 27, no. 21, pp. 29854–29862, Oct. 2019, doi: 10.1364/oe.27.029854.
- [9] B. Jain, R. T. Velpula, M. Patel, and H. P. T. Nguyen, “Controlled carrier mean free path for the enhanced efficiency of III-nitride deep-ultraviolet light-emitting diodes,” *Applied Optics*, vol. 60, no. 11, pp. 3088–3093, Apr. 2021, doi: 10.1364/ao.418603.
- [10] N. K. Manjunath, Y. Lu, and S. Lin, “Van der Waals contacted MoO<sub>x</sub> stacked ZnO/GaN vertical heterostructured ultraviolet light emitting diodes,” *Optics Express*, vol. 28, no. 21, pp. 31603–31610, Oct. 2020, doi: 10.1364/oe.402261.
- [11] D. Durmus and W. Davis, “Blur perception and visual clarity in light projection systems,” *Optics Express*, vol. 27, no. 4, pp. A216–A223, Feb. 2019, doi: 10.1364/oe.27.00a216.
- [12] W. Bao, M. Wei, and K. Xiao, “Investigating unique hues at different chroma levels with a smaller hue angle step,” *Journal of the Optical Society of America A*, vol. 37, no. 4, pp. 671–679, Apr. 2020, doi: 10.1364/josaa.383002.
- [13] H. Jiang *et al.*, “Projection optical engine design based on tri-color LEDs and digital light processing technology,” *Applied Optics*, vol. 60, no. 23, pp. 6971–6977, Aug. 2021, doi: 10.1364/AO.432355.
- [14] Z. Zhao, H. Zhang, S. Liu, and X. Wang, “Effective freeform TIR lens designed for LEDs with high angular color uniformity,” *Applied Optics*, vol. 57, no. 15, pp. 4216–4221, May 2018, doi: 10.1364/ao.57.004216.
- [15] I. G. Palchikova, E. S. Smirnov, and E. I. Palchikov, “Quantization noise as a determinant for color thresholds in machine vision,” *Journal of the Optical Society of America A*, vol. 35, no. 4, pp. B214–B222, Apr. 2018, doi: 10.1364/josaa.35.00b214.
- [16] S. An, J. Zhang, and L. Zhao, “Optical thermometry based on upconversion luminescence of Yb<sup>3+</sup>-Er<sup>3+</sup> and Yb<sup>3+</sup>-Ho<sup>3+</sup> doped Y<sub>6</sub>WO<sub>12</sub> phosphors,” *Applied Optics*, vol. 58, no. 27, pp. 7451–7457, Sep. 2019, doi: 10.1364/ao.58.007451.
- [17] T. DeLawyer, M. Tayon, C. Yu, and S. L. Buck, “Contrast-dependent red-green balance shifts depend on S-cone activity,” *Journal of the Optical Society of America A*, vol. 35, no. 4, pp. 114–121, Apr. 2018, doi: 10.1364/josaa.35.00b114.
- [18] W. Gao, K. Ding, G. He, and P. Zhong, “Color temperature tunable phosphor-coated white LEDs with excellent photometric and colorimetric performances,” *Applied Optics*, vol. 57, no. 31, pp. 9322–9327, Nov. 2018, doi: 10.1364/ao.57.009322.
- [19] V. M. Igba *et al.*, “Structural elucidation and optical properties of LiZrO<sub>2</sub>–LiBaZrO<sub>3</sub> nanocomposite doped with Mn<sup>2+</sup> ions,” *Optical Materials Express*, vol. 10, no. 11, pp. 2877–2895, Nov. 2020, doi: 10.1364/OME.402111.
- [20] L. Xie *et al.*, “Highly luminescent and stable lead-free cesium copper halide perovskite powders for UV-pumped phosphor-converted light-emitting diodes,” *Photonics Research*, vol. 8, no. 6, pp. 768–775, Jun. 2020, doi: 10.1364/prj.387707.
- [21] S. Matsumoto and A. Ito, “Chemical vapor deposition route to transparent thick films of Eu<sup>3+</sup>-doped HfO<sub>2</sub> and Lu<sub>2</sub>O<sub>3</sub> for luminescent phosphors,” *Optical Materials Express*, vol. 10, no. 4, pp. 899–906, Apr. 2020, doi: 10.1364/OME.386425.
- [22] X. Kong, M. J. Murdoch, I. Vogels, D. Sekulovski, and I. Heynderickx, “Perceived speed of changing color in chroma and hue directions in CIELAB,” *Journal of the Optical Society of America A*, vol. 36, no. 6, pp. 1022–1032, Jun. 2019, doi: 10.1364/josaa.36.001022.
- [23] C. Wu *et al.*, “Phosphor-converted laser-diode-based white lighting module with high luminous flux and color rendering index,” *Optics Express*, vol. 28, no. 13, pp. 19085–19096, Jun. 2020, doi: 10.1364/oe.393310.
- [24] A. R. Motschi *et al.*, “Identification and quantification of fibrotic areas in the human retina using polarization-sensitive OCT,” *Biomedical Optics Express*, vol. 12, no. 7, pp. 4380–4400, Jul. 2021, doi: 10.1364/boe.426650.
- [25] J.-H. Han *et al.*, “Improved efficiency of InGaN/GaN light-emitting diodes with perpendicular magnetic field gradients,” *Optics Express*, vol. 27, no. 25, pp. 36708–36716, Dec. 2019, doi: 10.1364/oe.27.036708.
- [26] R. Wan *et al.*, “Phosphor-free single chip GaN-based white light emitting diodes with a moderate color rendering index and significantly enhanced communications bandwidth,” *Photonics Research*, vol. 8, no. 7, pp. 1110–1117, Jul. 2020, doi: 10.1364/prj.392046.




- [27] H.-Y. Ryu, G.-H. Ryu, C. Onwukaeme, and B. Ma, "Temperature dependence of the Auger recombination coefficient in InGaN/GaN multiple-quantum-well light-emitting diodes," *Optics Express*, vol. 28, no. 19, pp. 27459–27472, Sep. 2020, doi: 10.1364/OE.402831.
- [28] Y. J. Sung *et al.*, "Light extraction enhancement of AlGaIn-based vertical type deep-ultraviolet light-emitting-diodes by using highly reflective ITO/Al electrode and surface roughening," *Optics Express*, vol. 27, no. 21, pp. 29930–29937, 2019, doi: 10.1364/oe.27.029930.

## BIOGRAPHIES OF AUTHORS



**Ha Thanh Tung**    received the Ph.D degree in physics from University of Science, Vietnam National University Ho Chi Minh City, Vietnam. He is working as a lecturer at the Faculty of Basic Sciences, Vinh Long University of Technology Education, Vietnam. His research interests focus on developing the patterned substrate with micro-and nano-scale to apply for physical and chemical devices such as solar cells, OLED, and photoanode. He can be contacted at email: tunght@vlute.edu.vn.



**Dieu An Nguyen Thi**    received a master of Electrical Engineering, HCMC University of Technology and Education, VietNam. Currently, she is a lecturer at the Faculty of Electrical Engineering Technology, Industrial University of Ho Chi Minh City, Vietnam. Her research interests are theoretical physics and mathematical physics. She can be contacted at email: nguyenthidieuan@iuh.edu.vn.